Geophys. J. Int. (1989) **98,** 23–38

A benchmark comparison for mantle convection codes

B. Blankenbach†, F. Busse‡, U. Christensen§, L. Cserepes¶,
D. Gunkel††, U. Hansen††, H. Harder§, G. Jarvis#,
M. Koch§§, G. Marquart¶¶, D. Moore*, P. Olson**
H. Schmeling†††† and T. Schnaubelt‡

† *Geophysikalisches Institut, Herzstraße* 16, 7500 *Karlsruhe, FRG*
‡ *Lehrstuhl IV für Theoretische Physik, Universität Bayreuth, Postfach* 2008, 8580 *Bayreuth, FRG*
§ *Max-Planck-Institut für Chemie, Saarstrasse* 23, 6500 *Mainz, FRG*
¶ *Geophysical Department, Eötvös University, Kun Béla ter.* 2, 1083 *Budapest, Hungary*
†† *Institut für Geophysik und Meteorologie, Universität Köln, Albertus-Magnus-Platz,* 5000 *Köln* 41, *FRG*
# *Department of Earth and Atmospheric Science, York University,* 4700 *Keele Street, North York, Ontario* M3J 1P3, *Canada*
§§ *Supercomputer Computations Research Institute and Department of Geology, Florida State University, Tallahassee,* FL 32306, *USA*
¶¶ *Institute of Geophysics, Department of Geodesy, Uppsala University, Hällby,* 75590 *Uppsala, Sweden*
* *Institute for Naval Oceanography, Stennis Space Center,* MI 39529-5005, *USA*
* *Permanent address: Department of Mathematics, Imperial College, London* SW7 2BZ, *UK.*
** *Department of Earth and Planetary Science, The Johns Hopkins University, Baltimore,* MD 21218, *USA*
†††† *Department of Mineralogy and Petrology, Uppsala University,* 75122 *Uppsala, Sweden*

Accepted 1988 December 16. Received 1988 July 18

SUMMARY

We have carried out a comparison study for a set of benchmark problems which are relevant for convection in the Earth's mantle. The cases comprise steady isoviscous convection, variable viscosity convection and time-dependent convection with internal heating. We compare Nusselt numbers, velocity, temperature, heat-flow, topography and geoid data. Among the applied codes are finite-difference, finite-element and spectral methods. In a synthesis we give best estimates of the 'true' solutions and ranges of uncertainty. We recommend these data for the validation of convection codes in the future.

Key words: mantle convection, numerical analysis, comparison of methods

1 INTRODUCTION

A major tool for understanding convection in the Earth's mantle is numerical analysis, simulation or computer experimentation. A large number of different numerical codes are used; however, relatively little is known about the advantages or disadvantages of the various methods. Another problem arises when a new code is set up and must be validated. Usually a published solution to some special problem is taken for a comparison. The accuracy of this solution is seldom known. Often numerical values are not available for a comparison and contour plots must be used, which have their own uncertainties. To overcome these problems benchmarks are common practice in other, more established, branches of computational physics. For one or a few well-defined problem(s), solutions are calculated with various codes, if possible using high resolution (i.e. large numerical grids) and considering the convergence behaviour with increasing degree of resolution. For example, a benchmark comparison has been organized by de Vahl-Davies & Jones (1983) for a standard convection problem at a Prandtl number of 0.71 (air). These published benchmarks are of limited interest for mantle convection codes, because of some major differences between standard problems in 'ordinary' fluid dynamics and solid state convection in planets. Some of the reasons are that in the latter case the Prandtl number is virtually infinite, whereas the variability of viscosity, rarely considered in fluid dynamics, is of greater interest. Another point relates to what aspects of the solution are studied. For mantle convection, the deflection of the free surface and the gravity signal are important quantities, since they are among the few observables which relate to the deep structure of convection. Their calculation requires higher derivatives of the dependent variable of the solution and are therefore especially sensitive to numerical errors.

The present benchmark study has been proposed in connection with a workshop on the numerical simulation of

Authors are listed in alphabetical order. Reprint requests should be directed to U. Christensen.

mantle convection, which took place in Neustadt/Weinstrasse (FRG) in 1987 June. Preliminary results were compared at the workshop and some extensions of the initial benchmark were decided upon. For example, only the Nusselt number and rms velocity were originally requested. There was a consensus that other, more localized, values of the solution should be included in the comparison. Now there are three groups of problems with a total of six cases in this benchmark. As the most basic problem, steady isoviscous convection in a square box heated from below is considered for various Rayleigh numbers. In the second group are two variable viscosity cases. As time-dependent aspects of convection have found a growing interest in recent years, the last case is one with intrinsically time-dependent behaviour.

After the original deadline for contributors had been extended, 10 individuals or groups finally joined into the venture, although few contributed to all cases, Still, we have a reasonably good coverage of most cases with different methods. A committee (U. Christensen, U. Hansen and H. Harder) has collected all contributions, summarized them and drafted a first version of this report. It was decided at the workshop that no rating of the codes should be stated in the report, but that we just let the results speak for themselves. We would even like to caution the reader who wants to do a rating for himself or herself. Many aspects have to be considered for such a rating. The most obvious one is that every convergent method would have given a better result if higher resolution had been used; therefore it is of no use to compare different methods when the degree of resolution also differs. Also, considering the level of accuracy for a given number of finite different points, finite elements or spectral modes, may not be the best standard of comparison, and comparing results obtained within a given CPU time on a standard computer would be better. Of course, this is not strictly possible (although CPU times are quoted in this report), because different machines have been used. A further aspect is that a code which does well in some aspects (e.g. gives a 'good' Nusselt number) may perform poorly in others (e.g. local temperatures). Further criteria may be important, for example the versatility of a code or the ease for implementing any alterations, but these are impossible to quantify.

In Section 2 we give the definition of the benchmark problems. In Section 3, the partaking numerical codes are briefly described. Section 4, consisting mainly of tables, contains all contributed results. In Section 5, we make an attempt to synthesize the results into best estimates for the exact solutions and the remaining level of uncertainty.

2 THE DEFINITION OF THE BENCHMARK CASES

2.1 General

We consider 2-D thermal convection of a non-rotating Boussinesq fluid of infinite Prandtl number in rectangular closed cells. Except for the viscosity in cases 2(a) and (b) all material properties are constant. Some definitions and notations are given in Table 1 along with dimensional reference values. However, except for topography and geoid

Table 1 Symbols and dimensional reference values

Symbol	Explanation	dimensional value (SI units)
x	horizontal coordinate, zero at left margin	
ℓ	length of cell	
z	vertical coordinate, positive upwards, zero at bottom	
h	height of cell	10^6
u, w	horizontal, vertical velocity	
T	temperature	
ΔT	temperature contrast (cases 1 and 2)	1000
ρ	density (Boussinesq-value)	4×10^3
κ	thermal diffusion constant	10^{-6}
g	gravity acceleration	10
α	thermal expansion coefficien:	2.5×10^{-5}
ν	kinematic viscosity	2.5×10^{19} (1a) 2.5×10^{18} (1b) 2.5×10^{17} (1c)
ν_0	kinematic viscosity at surface	2.5×10^{19}(2a,b)
c_p	heat capacity	1.25×10^3
Q	volumetric rate of internal heating (case 3)	5×10^{-9}
G	gravitational constant	6.673×10^{-11}
t	time	
ξ	surface/bottom topography	
ϕ	geoid anomaly	
q	temperature gradient	

non-dimensionalized data were requested. To remove the non-uniqueness all data are presented for the upwelling flow occurring at the left margin of the cell, i.e. at $x = 0$. The participants were encouraged to provide solutions obtained on different grids and to attempt to extrapolate their results. Apart from providing the data defined below, each participant was asked to give a brief description of the code, and give information about the machine used and the CPU time for the various cases.

2.2 Data to be calculated

The following five data or sets of data were to be calculated in cases 1(a)–(c) and 2(a) and (b). In case 3 only (i) and (ii) are requested.

(i) The Nusselt number

$$\mathrm{Nu} = -h \frac{\int_0^l \partial_z T(x, z = h)\, dx}{\int_0^l T(x, z = 0)\, dx}$$

(i.e. mean surface temperature gradient over mean bottom temperature).

Only in the time dependent case 3 is the use of this definition compulsory, in the other cases equivalent definitions of the Nusselt number could be used.

(ii) The (non-dimensional) rms velocity

$$v_{\mathrm{rms}} = \frac{h}{\kappa}\left\{\frac{1}{hl}\int_0^l \int_0^h (u^2 + w^2)\, dz\, dx\right\}^{1/2}.$$

(iii) Non-dimensional temperature gradients at the corners of the cell:

$$q = \frac{-h}{\Delta T}\left(\frac{\partial T}{\partial z}\right),$$

with

q_1 at $x = 0$, $z = h$; q_2 at $x = l$, $z = h$;

q_3 at $x = l$, $z = 0$; q_4 at $x = 0$, $z = 0$.

(iv) The depths (z_e) and values (T_e) of extrema of the temperature on the center-line ($x = l/2$, z). Only the extrema next to the upper and lower boundary are recorded. Scale the depth by h and temperature by ΔT.

(v) Topography of the free surface and bottom boundary and the geoid anomaly at the surface. These values are to be calculated at the cell margin $x = 0$ and $x = l$ in physical units (m) using the dimensional values in Table 1. Topography and geoid anomaly are normalized by setting the mean to zero. The position of the zero crossing (scaled by the height h) is also requested. Assume that there is no overlying medium (e.g. no water layer), and that the inviscid substratum has a density twice that of the convecting material (i.e. the density change is the same as for the upper surface).

ξ_1 surface topography at $x = 0$;
ξ_2 surface topography at $x = l$;
ξ_3 bottom topography at $x = 0$;
ξ_4 bottom topography at $x = l$;
Φ_1 geoid anomaly at $x = 0$, $z = h$;
Φ_2 geoid anomaly at $x = l$, $z = h$.

(vi) Additionally in case 3 the period of oscillations (if any were found) was requested, where time is scaled by h^2/κ.

2.3 Description of the benchmark cases

Case 1
Steady convection with constant viscosity in a square box ($l/h = 1$). Temperature is fixed to zero on top and to ΔT at the bottom, no internal heat sources. Reflecting symmetry at the sidewalls (i.e. $\partial_x T = 0$), zero shear stress on all boundaries. The Rayleigh number is $\mathrm{Ra} = \alpha g \Delta T h^3/\kappa\nu$
Case 1(a): $\mathrm{Ra} = 10^4$
Case 1(b): $\mathrm{Ra} = 10^5$
Case 1(c): $\mathrm{Ra} = 10^6$.

Case 2
Steady convection with temperature- and depth-dependent viscosity according to the equation

$$\nu = \nu_0 \exp\left[-\frac{bT}{\Delta T} + \frac{c(1-z)}{h}\right].$$

All boundary conditions as in case 1. The Rayleigh number is

$$\mathrm{Ra}_0 = \frac{\alpha g \Delta T h^3}{\kappa \nu_0}.$$

Case 2(a): Aspect ratio $l/h = 1$

$\mathrm{Ra}_0 = 10^4$

$b = \ln(1000) = 6.907755279$
$c = 0$.

Case 2(b): Aspect ratio $l/h = 2.5$

$\mathrm{Ra}_0 = 10^4$
$b = \ln(16384) = 9.704060528$

$c = \ln(64) = 4.158883083$.

Case 3
Time-dependent convection with constant viscosity and internal heating. The aspect ratio $l/h = 1.5$, the tangential velocity at the top and bottom boundary is zero (no slip condition). The top boundary is isothermal with $T = 0$, the temperature gradient $\partial T/\partial z$ at the bottom is zero. At the side walls there is reflective symmetry. The cell is homogeneously heated from within, and the Rayleigh number is

$$\mathrm{Ra} = \alpha g Q h^5/\kappa^2 \rho c_p \nu = 216\,000.$$

The initial condition is not prescribed; however, it should be chosen in order to obtain a single convection cell in the box. The evolution must be traced to that point where any transient behaviour has died away and (if possible) a strictly periodic regime is reached. Previous work (Lennie *et al.* 1988) has indicated that this system shows oscillatory time dependence due to instabilities in the upper boundary layer (growing blobs which are finally swept into the downwelling plume), and that it undergoes a sequence of period-doubling bifurcations between $\mathrm{Ra} = 190\,000$ and $220\,000$. This means that at lower Rayleigh numbers every blob behaves exactly in the same way (this is labelled a P1 cycle), at somewhat higher Rayleigh numbers only every second blob (P2 cycle), then every fourth blob (P4 cycle), etc. In time-series plots of Nu or v_{rms} the character of the cycle becomes obvious by comparing, for example, the maxima. At first they repeat identically, then pairs are identical, then quartetts and so on. In this case the following information was requested: the character of cycle, the period of a cycle and the maxima and minima of Nu and v_{rms}. From previous work it appeared likely that the transition point between the P2 and P4 cycle lies close to $\mathrm{Ra} = 216\,000$, therefore those who obtained a P2 cycle at this Rayleigh number were also asked to study the case with $\mathrm{Ra} = 218\,000$ (case 3′).

3 CODE DESCRIPTION

In our comparison study we have six finite-difference (FD) methods, three finite-element (FE) programs and one spectral approach. A brief description of each method is given in Table 2, with a reference for further reading for most codes. The majority of FD methods uses equidistant mesh spacing (except Cs and Ha), whereas the FE method naturally makes use of grid refinement in boundary layers. Because of the various ways of structuring non-equidistant grids we do not give more detailed information in this report other than numbers of points or elements. We think that for most of the requested data we have a sufficient diversity of methods included.

Table 2

Acronym	Author	Computer	Description of Method	Reference for Code
Bl	B. Blankenbach	Cyber 205	FE(NACHOS); 8-point-serendipity element, uwp, uw:quadratic, p:linear, T:quadratic, direct solver, time-dep: modified Crank-Nicholson, grid:ne	Gartling (1977)
Ko	M. Koch	Cyber 205	- same code as above, run independently, different grid structure -	" "
Ch	U. Christensen	CRAY XMP	FE; ψ:bicubic splines, T: biquadratic splines, upwind, direct solvers stat.: underrelaxation, time-dep: predictor-corrector, grid:ne	Christensen (1984)
Cs1	L. Cserepes	IBM 3031	FD; ψ : direct solver/SOR in case 2; T: upwind diff., ADI; grid:ne	Cserepes (1985)
Cs2	" "	" "	- same code as above, except with central diff.	" "
Ha	H. Harder	CRAY XMP	FD; ψ :direct solver; T:central diff., ADI; stat: underrelaxtion time-dep: predictor-correct.; grid:ne	-
HG	U. Hansen D. Gunkel	?	FE non-conforming element; ψ :quadratic; T: linear, upwind; direct solvers, stat: underrelax., time-dep.: predict-correct., grid: ne	Hansen & Ebel (1984)
Ja	G. Jarvis	IBM 4381	FD; ψ–ω implicit; T: explicit; grid: equi	
Mo	D. Moore	VAX 8800	FD; ψ-ω direct solv.; T:explicit (second order) DuFort-Frankel; grid: equi, staggered	Moore, Peckover & Weiss (1974)
Ol	P. Olson	Microvax	FD; ψ–ω or ψ, SOR; T: explicit (first order), Arakawa-Jacobian; grid: equi	-
SB	T. Schnaubelt F. Busse	Microvax	Spectral (Fourier), Galerkin, Newton-Raphson iter. (stat. only)	Busse (1967)
SM	H. Schmeling G. Marquardt	Comparex 8/85 Cyber 205	FD; ψ ; ADI; T: upwind (Spalding), ADI; stat.: relaxation, grid: equi	Schmeling & Jacoby (1981)

FE: finite element, FD: finite difference, ADI: alternating direction implicit meth., Ψ : stream-function (biharmonic eqn.)
ψ–ω : streamfunction vorticity approach, uwp= primitive variables, equi/ne = equidistant/nonequidist. mesh
stat: method to calculate stationary solutions

A few additional remarks will be given. All codes contributing to case 3 used some form of the Courant–Lewis–Friedrichs (CLF) criterion to control the time step. In some codes Δt was changed perpetually (HG, Ha), occasionally (Ch) or was fixed to a sufficiently low value to meet the CLF-criterion (Ko, Mo, SM). In cases 1 and 2 several workers (HG, Ch, Ko, Ha, Mo) preferred an average of advected and conducted heat flux through the whole cell to determine the Nusselt number, rather than the definition in Section 2. To determine temperature gradients, most FD methods used quadratic interpolation on three points (Mo tried various schemes). Temperature extrema were determined by a local quadratic fit of finite difference values, or by fitting all temperature values on the depth-profile by a cubic spline first, which Mo reported to give better results. All those contributing topography data calculated the vertical normal stress at the boundaries. This includes the determination of the dynamical pressure, which is only a variable of the solution in Ko. In the other approaches pressure was determined by integration of the Navier–Stokes equation, which involves calculation of third derivatives of the stream function (except in Ja, where vorticity is part of the solution). The integration path was along the surface in the code used by Ja, whereas Ch and Ha integrated first horizontally at some depth level and then vertically to the top or bottom boundary. SM reported results for both methods. The geoid was mostly (Ch, Ha, SM) calculated by a spectral method similar to Davis (1986). Ko used the method given by McKenzie, Roberts & Weiss (1974) to calculate the geoid at a height $z = 1.05h$, followed by downward continuation to the requested reference height $z = h$. For comparison, Ko also reported results obtained by the spectral technique. These data were tabulated under the entry Ko′. Additionally, Ch determined topography and geoid in constant viscosity cases by a Green's function integration of the temperature field (Parsons & Daly 1983), these solutions are labelled Ch′ in Tables 3(b), 4(b) and 5(b). Many authors attempted an extrapolation of results obtained with various degrees of resolution, as requested, although by different methods. Some (Ja, SM) used graphical methods or estimated an extrapolated value. Ha, HG, Mo used the Romberg scheme assuming a convergence order of two (plus higher *even* terms in the series expansion of the discretization error), and Cs took a related approach. Ch used Aitken extrapolation, which determines the exponent of the error term from the three results with highest resolution.

The participants had been asked if they would make their codes available upon request. There are affirmative answers from all participants, but almost all mentioned that there is poor documentation or none at all.

4 RESULTS

All contributed results are listed in Tables 3–5 for the constant viscosity case, Tables 6 and 7 for the variable viscosity problems and in Table 8 for the time-dependent case. Authors are listed in alphabetical order, except that Ko follows directly after Bl, because the code is identical and only the grids are different. Because of the symmetry of the solution in cases 1(a)–(c) we list only the non-redundant values, the others are recovered by the relations $q_3 = q_1$, $q_4 = q_2$, $T'_e = 1 - T_e$, $z'_e = 1 - z_e$, $\xi_3 = \xi_1$, $\xi_4 = \xi_2$.

Table 3a: Nusselt Number and other quantities for $Ra = 10^4$ (case 1a). Here, as in the following tables, the first number quoted under the entry 'grid' is the number of finite elements, finite difference intervals, or Fourier modes in x-direction; the second number the same in z-direction. 'Ext.' indicates an extrapolated result. CPU states the required computer time in seconds.

Code	Grid	Nu	v_{rms}	q_1	q_2	T_e	z_e	CPU
Bl	12x12	4.900	42.879	11.315	0.829	0.423	0.229	?
	24x24	4.888	42.865	9.630	0.704	0.422	0.225	?
Ko	16x16	4.892	42.87	—	—	—	—	30
	20x20	4.889	42.87	—	—	—	—	?
	28x28	4.887	42.87	—	—	—	—	?
Ch	12x12	4.888051	42.88511	8.063789	0.589369	0.426194	0.242738	0.42
	18x18	4.885027	42.86870	8.060111	0.588770	0.423347	0.231566	1.00
	24x24	4.884605	42.86617	8.059624	0.588787	0.422621	0.228503	1.95
	36x36	4.884451	42.86521	8.059440	0.588804	0.422269	0.226564	6.50
	48x48	4.884424	42.86504	8.059406	0.588808	0.422194	0.225888	15.4
	72x72	4.884412	42.86497	8.059390	0.588810	0.422163	0.225350	?
	ext.	4.884407	42.86495	8.059383	0.588811	0.422155	0.224787	—
Cs1	36x36	4.896	42.82	8.204	0.810	0.4271	0.2425	556.
Cs2	36x36	4.867	42.84	8.076	0.634	0.4221	0.2279	629.
Ha	16x16	4.854089	42.461608	7.676221	0.583318	0.41248	0.21794	0.23
	32x32	4.876425	42.766185	7.960992	0.586992	0.42052	0.22505	1.04
	48x48	4.880784	42.821218	8.015463	0.587974	0.42156	0.22491	2.81
	72x72	4.882773	42.845543	8.039826	0.588437	0.42185	0.22493	8.30
	ext.	4.884391	42.864944	8.059383	0.588819	0.42209	0.22495	—
HG	12x12	4.93529	43.316	7.97295	0.53968	—	—	5.
	18x18	4.90712	43.071	8.03526	0.56789	—	—	11.
	24x24	4.89721	42.983	8.04949	0.57734	0.42063	0.2237	20.
	ext.	4.88443	42.870	8.0620	0.58917	—	—	—
Ja	12x12	4.565	40.79	5.824	0.8031	0.4308	0.250	?
	24x24	4.804	42.36	6.865	0.646	0.4264	0.25	?
	48x48	4.864	42.74	7.841	0.604	0.4229	0.2292	?
	ext.	4.884	42.87	8.166	0.590	0.4217	0.2292	—
Mo	12x12	4.649818	42.296484	7.515712	0.893869	0.429987	0.239896	15
	24x24	4.827453	42.740465	8.209264	0.657167	0.424393	0.228939	60
	48x48	4.870284	42.834928	8.152498	0.605460	0.422741	0.225899	300
	96x96	4.880885	42.857510	8.087722	0.592947	0.422308	0.225154	4.5×10^3
	192x192	4.883529	42.863093	8.066821	0.589843	0.422199	0.224967	6.0×10^4
	384x384	4.884189	42.864484	8.061267	0.589068	0.422171	0.224919	2.7×10^6
	ext.	4.884409	42.864947	8.059386	0.588810	0.422162	0.224903	—
Ol	11x11	5.189	44.69	8.75	0.533	0.40	0.20	30.
	31x31	4.90	43.10	8.44	0.582	0.419	0.233	1400.
SB	20x20	4.88441	—	—	—	—	—	?
	30x30	4.88441	42.86493	8.059384	0.5888102	—	—	?
	34x34	4.88441	42.86493	8.059384	0.5888102	0.42216	0.225	?
SM	41x41	4.866	42.802	8.00	0.60	0.421	0.225	27.5

Table 3b: Topography and geoid for $Ra = 10^4$ (case 1a)

Code	Grid	ξ_1	ξ_2	$x(\xi = 0)$	Φ_1	Φ_2	$x(\Phi = 0)$
Ch	12x12	2232.417	-2871.356	0.537911	54.3110	-61.8028	0.518744
	18x18	2244.283	-2889.216	0.538525	54.5951	-62.2678	0.519210
	24x24	2248.580	-2895.441	0.538852	54.6947	-62.4251	0.519396
	36x36	2251.627	-2899.814	0.539134	54.7654	-62.5354	0.519531
	48x48	2252.682	-2901.322	0.539247	54.7900	-62.5737	0.519579
	72x72	2253.430	-2902.387	0.539315	54.8077	-62.6008	0.519613
	ext.	2254.021	-2903.221	0.539377	54.8223	-62.6220	0.519639
Ch'	18x18	2254.092	-2903.312	0.539386	54.8248	-62.6268	0.519644
	36x36	2254.027	-2903.233	0.539373	54.8221	-62.6228	0.519640
	72x72	2254.023	-2903.229	0.539372	54.8219	-62.6226	0.519640
Ha	16x16	2215.309	-2877.700	0.53923	54.04341	-62.39527	0.52031
	32x32	2244.122	-2897.856	0.53932	54.62259	-62.57810	0.51979
	48x48	2249.597	-2900.930	0.53934	54.73283	-62.60385	0.51971
	72x72	2252.050	-2902.225	0.53936	54.78218	-62.61444	0.51967
	ext.	2254.023	-2903.230	0.53937	54.82184	-62.62252	0.51964
Ja	12x12	2017.	-2449.	0.5325	—	—	—
	24x24	2188.	-2775.	0.5374	—	—	—
	48x48	2237.	-2869.	0.5390	—	—	—
	ext.	2253.	-2900.	0.5395	—	—	—
Ko	16x16	2311.	-2849.	0.548	56.112	-61.220	0.528
	20x20	2309.	-2851.	0.548	56.115	-61.287	0.528
	28x28	2306.	-2852.	0.548	56.090	-61.343	0.528
Ko'	16x16	—	—	—	55.116	-60.059	0.528
	20x20	—	—	—	55.183	-60.159	0.528
	28x28	—	—	—	55.406	-60.534	0.528
SM	41x41	2270.	-2899.	0.5403	55.311	-62.812	0.5244

Table 4a: Nusselt Number and other quantities for Ra= 10^5 (case 1b)

Code	Grid	Nu	v_{rms}	q_1	q_2^*	T_e	z_e	CPU
Bl	12x12	10.611	193.378	26.302	1.018	0.4223	0.115	?
	18x18	10.556	193.237	23.370	0.959	0.429	0.115	?
Ko	16x16	10.565	193.25	—	—	—	—	30
	20x20	10.561	193.23	—	—	—	—	?
	28x28	10.542	193.20	—	—	—	—	?
Ch	18x18	10.537808	193.24869	—	—	—	—	1.00
	24x24	10.534872	193.22056	—	—	—	—	1.95
	36x36	10.534198	193.21516	19.079543	0.722755	0.428330	0.113476	6.50
	48x48	10.534127	193.21471	19.079476	0.722752	0.428298	0.111100	15.4
	72x72	10.534102	193.21456	19.079458	0.722751	0.428379	0.111955	68.2
	ext.	10.534095	193.21449	19.079449	0.722751	0.428426	0.111700	—
Cs1	36x36	10.45	194.3	19.35	1.45	0.4366	.1288	1326.
Ha	16x16	10.21010	187.88514	17.62524	0.7087698	0.42554	0.11436	0.28
	32x32	10.45222	191.85834	18.71108	0.7180809	0.42708	0.11118	1.50
	48x48	10.49766	192.61007	18.91559	0.7206500	0.42718	0.11123	4.41
	72x72	10.51789	192.94554	19.00660	0.7218345	0.42805	0.11178	11.2
	ext.	10.53409	193.21449	19.07944	0.7228010	0.4287	0.1122	—
HG	18x18	10.6136	193.79	18.890	0.6765	—	—	5.
	24x24	10.5870	193.71	19.001	0.6948	0.4245	0.1102	11.
	36x36	10.5597	193.53	19.0570	0.7109	—	—	12.
	ext.	10.5330	193.31	19.0878	0.7256	—	—	—
Ja	24x24	10.028	189.7	17.69	1.109	0.4397	0.1250	?
	48x48	10.417	192.4	16.63	0.825	0.4333	0.1042	?
	96x96	10.504	193.1	18.37	0.749	0.4293	0.1146	?
	ext.	10.533	193.33	18.95	0.724	0.4280	0.1146	—
Mo	12x12	8.522998	180.339114	11.422313	2.955357	0.452454	0.140574	15
	24x24	10.070902	190.921598	16.962470	1.189592	0.438850	0.118054	80
	48x48	10.422827	192.714652	19.428339	0.833373	0.431359	0.113527	470
	96x96	10.506561	193.094088	19.401945	0.750409	0.429184	0.112222	$6.5\text{x}10^3$
	192x192	10.527229	193.184711	19.184495	0.729671	0.428618	0.111910	$4.3\text{x}10^4$
	384x384	10.532380	193.207101	19.107472	0.724482	0.428475	0.111830	$3.7\text{x}10^5$
	ext.	10.534095	193.214540	19.079522	0.722751	0.428427	0.111804	?
Ol	43x43	10.63	196.48	20.76	0.689	0.422	0.12	$6.\text{x}10^3$
	53x53	10.54	194.15	20.44	0.698	0.424	0.115	$1.\text{x}10^4$
SB	20x20	10.49047	—	—	—	—	—	?
	30x30	10.53309	193.2124	18.94788	0.7565370	—	—	?
	34x34	10.53383	193.2142	19.03325	0.7312343	—	—	?
	38x38	10.53402	193.2143	19.06459	0.7248052	0.42842	0.112	?
SM	31x31	10.733	202.23	—	—	—	—	24.
	41x41	10.6921	197.96	18.80	0.68	0.415	0.10	48.
	51x51	10.6254	195.85	—	—	—	—	?
	61x61	10.583	194.68	—	—	—	—	?
	ext.	10.5	192.	—	—	—	—	—

Table 4b: Topography and geoid for Ra= 10^5 (case 1b)

Code	Grid	ξ_1	ξ_2	$x(\xi=0)$	Φ_1	Φ_2	$x(\Phi=0)$
Ch	18x18	1457.066	-1999.334	0.530602	27.7928	-32.1637	0.513688
	24x24	1458.692	-2001.235	0.529908	27.7462	-32.0867	0.513035
	36x36	1459.981	-2002.850	0.529535	27.7197	-32.0434	0.512606
	48x48	1460.426	-2003.438	0.529431	27.7116	-32.0302	0.512465
	72x72	1460.739	-2003.862	0.529377	27.7063	-32.0215	0.512368
	ext.	1460.986	-2004.205	0.529342	27.7026	-32.0155	0.512290
Ch'	18x18	1461.338	-2004.632	0.529498	27.7063	-32.0160	0.512277
	36x36	1460.982	-2004.209	0.529321	27.7024	-32.0151	0.512292
	72x72	1460.988	-2004.206	0.529323	27.7025	-32.0153	0.512294
Ha	16x16	1456.510	-1974.860	0.52788	26.83919	-30.94725	0.51149
	32x32	1460.086	-1997.144	0.52885	27.47497	-31.73502	0.51207
	48x48	1460.675	-2001.209	0.52911	27.60199	-31.89339	0.51220
	72x72	1460.859	-2002.864	0.52923	27.65745	-31.96051	0.51225
	ext.	1461.00	-2004.18	0.52933	27.7018	-32.0142	0.51229
Ja	24x24	1355.	-1779.	0.5315	—	—	—
	48x48	1430.	-1942.5	0.5306	—	—	—
	96x96	1452.2	-1988.0	0.5297	—	—	—
	ext.	1460.	-2003.	0.5294	—	—	—
Ko	16x16	1507.	-1964.	0.541	28.208	-31.178	0.523
	20x20	1504.	-1965.	0.548	28.258	-31.311	0.524
	28x28	1501.	-1966.	0.548	28.278	-31.394	0.523
Ko'	16x16	—	—	—	28.989	-32.015	0.523
	20x20	—	—	—	28.580	-31.580	0.522
	28x28	—	—	—	28.524	-31.584	0.522
SM	31x31	1524.	-2109.	—	28.87	-33.46	—
	41x41	1503.	-2059.	0.5308	28.36	-32.75	0.5125
	51x51	1488.	-2034.	—	28.08	-32.39	—
	61x61	1477.	-2020.	0.5294	27.93	-32.20	0.5121
	ext.	1450.	-1990.	—	27.6	-31.85	—

Table 5a: Nusselt Number and other quantities for Ra 10^6 (case 1c)

Code	Grid	Nu	v_{rms}	q_1	q_2	T_e	z_e	CPU
Bl	18x18	22.095	834.442	55.458	1.110	0.428	0.060	?
	24x24	22.011	834.076	53.649	1.047	0.431	0.060	?
Ko	16x16	22.213	834.79	—	—	—	—	30
	20x20	22.048	834.23	—	—	—	—	?
	28x28	21.997	834.02	—	—	—	—	?
Ch	18x18	21.992493	834.33915	45.992086	0.880186	0.439219	0.061290	1.08
	24x24	21.975848	834.09767	45.982865	0.876882	0.430885	0.059659	2.12
	36x36	21.973095	834.00705	45.969043	0.877142	0.432728	0.058195	7.1
	48x48	21.972682	833.99512	45.966229	0.877159	0.432052	0.057907	16.9
	72x72	21.972520	833.99090	45.964848	0.877167	0.432264	0.057792	70.
	ext.	21.972467	833.98973	45.964237	0.877170	0.4322	0.057762	—
Cs1	36x36	21.57	844.5	46.97	3.04	0.4459	0.0735	1760.
Ha	32x32	21.79339	826.2476	45.35191	0.878980	0.42970	0.058270	2.77
	48x48	21.89232	830.5180	45.69387	0.878092	0.43103	0.057919	5.62
	72x72	21.93675	832.4402	45.84449	0.877372	0.43182	0.057754	12.6
	ext.	21.97251	833.9889	45.96437	0.87665	0.4324	0.05762	—
HG	18x18	22.270	836.77	40.610	0.6752	—	—	5.
	24x24	22.165	836.55	43.243	0.7629	0.4220	0.0568	11.
	36x36	22.065	835.55	44.891	0.8271	—	—	12.
	ext.	21.970	834.24	46.069	0.8794	—	—	—
Ja	48x48	21.075	824.4	27.20	1.524	0.444	0.0625	?
	64x64	21.482	829.0	32.05	1.255	0.4398	0.0625	?
	96x96	21.76	832.2	37.89	1.054	0.4365	0.0625	?
	ext.	21.98	834.76	42.56	0.893	0.4339	0.0625	—
Mo	24x24	17.952049	777.409478	24.411426	4.824588	0.457322	0.069257	290
	48x48	21.077723	823.739556	37.490874	1.605908	0.443698	0.060427	2300
	96x96	21.759416	831.732658	46.103451	1.063390	0.435380	0.058434	$2.3x10^4$
	192x192	21.919836	833.443892	46.959928	0.925027	0.433019	0.057916	$1.4x10^5$
	384x384	21.959351	833.854447	46.334472	0.889231	0.432408	0.057784	$1.0x10^6$
	ext.	21.972470	833.989766	46.030080	0.877165	0.432202	0.057740	—
Ol	61x61	22.18	842.5	49.4	0.755	0.428	0.067	$3.x10^4$
	81x81	21.978	834.67	50.09	0.812	0.427	0.0625	$7.2x10^4$
SB	24x24	19.31557	—	—	—	—	—	?
	32x32	20.98983	817.9426	35.37384	8.67458	—	—	?
	38x38	21.53851	827.0860	38.90709	6.31983	—	—	?
	44x44	21.79208	831.2253	41.40324	4.29647	0.43094	0.058	?
SM	31x31	17.348	979.89	—	—	—	—	19.
	41x41	20.081	912.74	29.8	0.68	0.376	0.05	40.
	51x51	21.889	886.76	—	—	—	—	123.
	61x61	22.792	875.30	—	—	—	—	217.
	ext.	23.	855.	—	—	—	—	—

Table 5b: Topography and geoid for Ra=10^6 (case 1c)

Code	Grid	ξ_1	ξ_2	$x(\xi = 0)$	Φ_1	Φ_2	$x(\Phi = 0)$
Ch	18x18	934.282	-1285.199	0.508009	13.6952	-15.3588	0.502435
	24x24	932.905	-1284.371	0.507345	13.5780	-15.2029	0.501548
	36x36	932.333	-1284.015	0.506880	13.5047	-15.1047	0.500920
	48x48	932.162	-1283.908	0.506713	13.4807	-15.0725	0.500701
	72x72	932.048	-1283.845	0.506594	13.4642	-15.0504	0.500544
	ext.	931.962	-1283.813	0.506498	13.4520	-15.0340	0.500416
Ch'	18x18	932.476	-1284.671	0.506484	—	—	—
	36x36	931.962	-1283.824	0.506498	13.4516	-15.0334	0.500418
	72x72	931.961	-1283.804	0.506500	13.4515	-15.0333	0.500419
Ha	32x32	935.119	-1280.22	0.50683	13.2742	-14.7949	0.50040
	48x48	933.382	-1282.28	0.50664	13.3819	-14.9423	0.50049
	72x72	932.574	-1283.13	0.50655	13.4129	-14.9810	0.50039
	ext.	931.927	-1283.79	0.50647	13.4376	-15.0120	0.50039
Ja	48x48	875.	-1169.	0.5131	—	—	—
	64x64	896.	-1217.	0.5113	—	—	—
	96x96	914.	-1253.	0.5091	—	—	—
	ext.	928.	-1282.	0.5073	—	—	—
Ko	16x16	966.6	-1271.	0.530	13.786	-14.599	0.487
	20x20	960.4	-1267.	0.531	13.695	-14.752	0.499
	28x28	955.4	-1265.	0.530	13.650	-14.858	0.505
Ko'	16x16	—	—	—	15.376	-16.563	0.504
	20x20	—	—	—	14.410	-15.564	0.505
	28x28	—	—	—	14.198	-15.419	0.504
SM	31x31	1008.	-1490.	—	15.82	-17.72	—
	41x41	973.2	-1413.	—	14.76	-16.18	—
	51x51	977.3	-1379.	—	14.37	-16.03	—
	61x61	992.7	-1358.	—	14.21	-15.80	—
	ext.	1020.	-1320.	—	13.9	-15.25	—

Table 6a: Nusselt Number and other quantities for temperature-dependent rheology (case 2a)

Code	Grid	Nu	v_{rms}	q_1	q_2	q_3	q_4	T_e	z_e	T_e	z_e	CPU
Bl	18x18	9.576	478.036	20.103	1.377	31.215	0.597	0.756	0.063	0.854	0.818	?
	24x24	9.630	483.030	17.332	1.156	25.854	0.510	0.753	0.063	0.846	0.818	?
Ko	16x16	9.496	476.95	—	—	—	—	—	—	—	—	?
	20x20	9.667	478.63	—	—	—	—	—	—	—	—	?
	28x28	9.849	479.78	—	—	—	—	—	—	—	—	150.
Ch	18x18	10.06681	480.7714	17.53909	1.015290	26.79242	0.497214	0.742056	0.067577	0.830956	0.842760	2.94
	24x24	10.06738	480.3088	17.52025	1.008742	26.82805	0.497334	0.739915	0.062210	0.831646	0.832593	5.82
	36x36	10.065863	480.38728	17.52924	1.008509	26.81372	0.497356	0.740435	0.063225	0.832293	0.829998	19.4
	48x48	10.065907	480.41558	17.53059	1.008513	26.81125	0.497373	0.740599	0.062712	0.832381	0.826806	47.4
	72x72	10.065949	480.42971	17.53116	1.008511	26.80979	0.497379	0.740475	0.062492	0.832376	0.824409	190.
	ext.	10.065995	480.43342	17.53136	1.008509	26.80846	0.497380	0.740450	0.062424	0.832350	0.823	—
Cs1	23x23	10.61	524.2	—	—	—	—	—	—	—	—	?
	33x33	10.38	503.3	19.25	1.77	27.68	1.96	0.7161	0.0797	0.7955	0.8132	1208.
	ext.	9.90	468.3	—	—	—	—	—	—	—	—	—
Cs2	23x23	10.35	446.1	—	—	—	—	—	—	—	—	?
	33x33	10.19	458.3	19.31	0.92	25.41	0.42	0.7239	0.0676	0.8200	0.8232	2888.
	ext.	10.04	469.8	—	—	—	—	—	—	—	—	—
Ha	24x24	9.93096	478.232	17.8744	1.01904	25.5240	0.487645	0.72873	0.063329	0.82746	0.83359	8.45
	48x48	10.0379	480.620	17.6282	1.01095	26.5374	0.494881	0.73757	0.062550	0.83084	0.82548	40.9
	72x72	10.0543	480.622	17.5759	1.00956	26.6941	0.496243	0.73922	0.062426	0.83161	0.82481	133.
	ext.	10.0667	480.524	17.5325	1.00847	26.8124	0.49733	0.74053	0.062331	0.83222	0.82428	—
HG	24x24	10.0686	482.53	17.2714	0.98884	20.24074	0.30503	0.74189	0.061770	0.840762	0.82137	130.
	36x36	10.0678	479.56	17.549	1.0032	25.67385	0.46006	—	—	—	—	?
	ext.	10.0671	477.18	17.7711	1.0147	30.0203	0.58408	—	—	—	—	—
SM	31x31	9.07	453.0	13.62	1.20	13.98	0.33	0.6563	0.0708	0.8472	0.7966	435.
	41x41	9.63	454.5	14.76	1.12	17.48	0.40	0.6800	0.0625	0.8393	0.8083	1126.
	51x51	9.88	464.2	15.55	1.10	20.7	0.45	0.7024	0.0635	0.8403	0.8133	1500.
	61x61	9.93	473.9	—	—	—	—	—	—	—	—	?
	ext.	10.5	482.	—	—	—	—	—	—	—	—	—

Table 6b: Topography and geoid for temperature-dependent rheology (case 2a)

Code	Grid	ξ_1	ξ_2	$x(\xi = 0)$	ξ_3	ξ_4	$x(\xi = 0)$	Φ_1	Φ_2	$x(\Phi = 0)$
Ch	18x18	1017.74	-4090.67	0.676680	388.27	-788.45	0.632959	17.808	-54.971	0.657272
	24x24	1015.084	-4094.314	0.677194	387.435	-788.770	0.631710	17.6252	-54.8676	0.658486
	36x36	1012.871	-4096.258	0.677133	386.879	-788.208	0.631285	17.4673	-54.7169	0.659316
	48x48	1011.974	-4097.046	0.677068	386.660	-788.144	0.631102	17.4122	-54.6643	0.659592
	72x72	1011.326	-4097.627	0.677025	386.499	-788.112	0.630958	17.3775	-54.6278	0.659784
	ext.	1010.925	-4098.073	0.677001	386.373	-788.086	0.630840	17.3430	-54.5984	0.659931
Ha	24x24	1016.75	-3850.45	0.66811	398.618	-876.950	0.63360	16.9181	-51.3051	0.65503
	48x48	1012.87	-4033.43	0.67477	389.432	-817.392	0.63210	17.2468	-53.7822	0.65873
	72x72	1011.82	-4069.36	0.67602	387.742	-801.830	0.63149	17.3026	-54.2411	0.65941
	ext.	1010.90	-4098.56	0.67702	386.393	-788.362	0.63093	17.3461	-54.6082	0.65995
Ko	16x16	1232.	-3696.	0.758	416.7	-673.8	0.727	16.67	-52.06	0.670
	20x20	1256.	-3717.	0.761	421.2	-692.2	0.726	16.91	-52.26	0.668
	28x28	1284.	-3744.	0.761	426.4	-713.5	0.723	17.42	-53.28	0.667
Ko'	16x16	—	—	—	—	—	—	18.40	-53.55	0.654
	20x20	—	—	—	—	—	—	18.03	-53.35	0.654
	28x28	—	—	—	—	—	—	18.07	-53.83	0.659
SM	31x31	1297.6	-3516.2	0.7075	1879.4	-126.4	0.5430	17.97	-52.68	0.6585
	41x41	1160.6	-3783.3	0.6977	1428.7	-448.5	0.5948	17.56	-52.29	0.6591
	51x51	1092.9	-3895.9	0.6918	1100.2	-564.6	0.6151	17.13	-52.32	0.6580
	ext.	1000.	-4050.	0.675	(400)	(-900)	0.67	16.	-52.4	0.6585

Table 7a: Nusselt Number and other quantities for temperature- and depth-dependent rheology (case 2b)

Code	Grid	Nu	v_{rms}	q_1	q_2	q_3	q_4	T_e	z_e	T_e	z_e	CPU
Bl	18x18	6.795	170.223	20.598	0.246	17.118	0.792	0.413	0.187	0.598	0.783	?
	24x24	6.836	171.568	17.496	0.215	14.979	0.668	0.415	0.187	0.599	0.779	?
Ko	16x16	6.749	169.59	—	—	—	—	—	—	—	—	80.
	20x20	6.822	170.61	—	—	—	—	—	—	—	—	?
	28x28	6.876	171.16	—	—	—	—	—	—	—	—	?
Ch	36x18	6.958129	172.9789	—	—	—	—	—	—	—	—	5.0
	48x24	6.933153	171.89687	18.50291	0.177529	14.16516	0.617438	0.398288	0.196584	0.577376	0.773536	10.7
	72x36	6.930056	171.76533	18.48383	0.177462	14.17037	0.617670	0.397281	0.193156	0.576338	0.783011	37.5
	96x48	6.929978	171.76540	18.48420	0.177443	14.17015	0.617689	0.397099	0.192048	0.575940	0.786534	91.
	ext.	6.929913	171.76540	18.48774	0.177426	14.17005	0.617700	0.397099	0.190809	0.575833	0.782726	—
Cs1	50x25	7.409	193.1	21.85	0.45	15.09	1.96	0.4026	0.2053	0.5635	0.7650	3760
Cs2	50x25	6.806	166.7	19.93	0.17	13.59	0.22	0.3849	0.1995	0.5608	0.7647	5410
Ha	32x32	6.86187	167.718	18.7519	0.173788	14.0444	0.606305	0.38799	0.19346	0.56683	0.77418	54.
	48x48	6.89925	169.951	18.6016	0.175805	14.1142	0.612699	0.39313	0.19251	0.57182	0.77965	195.
	72x72	6.91611	170.950	18.5360	0.176701	14.1444	0.615494	0.39528	0.19139	0.57405	0.78195	480.
	ext.	6.92970	171.753	18.4842	0.177417	14.1682	0.617708	0.39695	0.19049	0.57585	0.78373	—
HG	18x18	6.9948	177.17	16.7309	0.1529	13.9595	0.3059	0.4067	0.1853	0.6032	0.7897	84.
	24x24	6.9692	174.793	17.4181	0.1634	14.0350	0.4271	0.4032	0.1870	0.5922	0.7863	150.
	ext.	6.9360	171.73	17.9678	0.1717	14.0954	0.5241	—	—	—	—	—
SM	41x41	8.16	246.0	17.00	0.28	14.92	0.28	0.4860	0.150	0.7540	0.825	208
	41x21	7.43	242.	12.26	0.36	11.84	0.26	0.4812	0.1426	0.7771	0.8226	160
	61x31	7.40	212.	14.46	0.30	13.44	0.42	0.4681	0.1577	0.7038	0.8166	240
	81x41	7.38	208.5	15.48	0.28	14.44	0.48	0.4704	0.160	0.6820	0.8125	700
	ext.	7.35	195.	17.0	0.27	16.6	0.60	0.47	0.165	0.650	0.805	—

Table 7b: Topography and geoid for temperature- and depth-dependent rheology (case 2b)

Code	Grid	ξ_1	ξ_2	$x(\xi = 0)$	ξ_3	ξ_4	$x(\xi = 0)$	Φ_1	Φ_2	$x(\Phi = 0)$
Ch	36x18	1553.48	-4351.20	1.637742	2306.90	-6649.13	1.739081	-10.473	-29.540	1.274083, 2.297762
	48x24	1553.198	-4340.227	1.636845	2314.014	-6630.167	1.732345	-11.2758	-28.6508	1.274575, 2.302927
	72x36	1544.948	-4340.706	1.636218	2313.209	-6634.261	1.731361	-11.5676	-28.4401	1.274653, 2.304748
	96x48	1542.246	-4341.180	1.636016	2312.654	-6636.745	1.731248	-11.6583	-28.3738	1.274767, 2.305338
	ext.	1540.200	-4341.474	1.635803	2311.821	-6639.780	1.731084	-11.7759	-28.2782	1.274881, 2.306150
Ha	32x32	1579.63	-4311.23	1.6256	2319.70	-6453.48	1.7197	-9.8094	-31.8617	1.2411, 2.2822
	48x48	1557.20	-4329.81	1.6378	2315.05	-6555.95	1.7258	-10.8030	-29.9932	1.2605, 2.2951
	72x72	1547.03	-4336.92	1.6344	2313.19	-6601.85	1.7288	-11.3963	-29.0285	1.2683, 2.3014
	ext.	1538.81	-4342.09	1.6344	2311.80	-6638.73	1.7312	-11.9381	-28.1971	1.2742, 2.3066
Ko	16x16	2131.	-3861.	1.970	2946.	-6133.	1.905	-13.01	-26.78	1.296, 2.327
	20x20	2158.	-3802.	1.965	2935.	-6079.	1.895	-12.35	-27.59	1.285, 2.320
	28x28	2184.	-3739.	1.974	2920.	-6088.	1.882	-11.81	-28.07	1.274, 2.313
Ko'	16x16	—	—	—	—	—	—	-10.41	-28.11	1.312, 2.320
	20x20	—	—	—	—	—	—	-11.90	-26.58	1.308, 2.323
	28x28	—	—	—	—	—	—	-11.26	-26.98	1.298, 2.316
SM	41x21	2379.	-6355.	1.796	4730.	-8269.	1.796	-2.47	-44.2	1.3751, 2.3617
	61x31	1736.	-5554.	1.7503	2675.	-7940.	1.805	-4.92	-39.1	1.3600, 2.3364
	81x41	1526.	-5399.	1.7322	2280.	-7778.	1.810	-7.40	-38.2	1.3401, 2.331
	ext.	1300.	-4800.	1.705	1800.	-7100.	1.825	-13.0	-36.	1.30, 2.32

A remark is appropriate concerning the vast differences in tablulated CPU-time for about equal grid size. They mainly reflect differences in computational speed, which, according to the 'Linpack benchmark' (Dongara 1986) relate, for example, like 350:7:1 for the CRAY XMP, VAX 8800 and Microvax II. A second point is that some use an iteration method to find a steady state, whereas others use real time steps. The second method usually takes much longer, however, it has the advantage to ensure the stability of the final steady solution against time-dependent disturbances.

In the constant viscosity case the agreement is excellent for the global properties Nu and v_{rms}, even at $Ra = 10^6$. The individual best resolved results agree for all codes within 1–2 per cent. We show the convergence behaviour at $Ra = 10^6$ for all codes in Fig. 1, where results are plotted versus $\sqrt{N^{-1}}$, with N being the total number of finite

Table 8: Nusselt Number, velocity(rms) and period in the time-dependent problem (case 3)

Code	Grid	Type	Period	Nusselt Nu. max	Nusselt Nu. min	velocity(rms) max	velocity(rms) min	max	min	CPU per timestep
Ch	24x16	P2	0.048125	7.41120	6.48660	7.22407	6.81599	60.4349	31.9424	57.5174	30.2854	0.080
	36x24	P2	0.048066	7.38809	6.47424	7.20315	6.80255	60.3737	31.9652	57.4470	30.3057	0.210
	50x32	P2	0.048052	7.38252	6.47106	7.19940	6.79887	60.3680	31.9725	57.4358	30.3128	0.702
	ext.		0.048043	7.37845	6.46740	7.19712	6.79493	60.3674	31.9785	57.4309	30.3160	—
Cs1	48x24	chaotic		—	—	—	—		—	—	—	2.34
Ha	36x24	P4	0.09326	7.404	6.446	7.223	6.778	64.21	33.15	60.80	31.18	
				7.406	6.419	7.169	6.746	63.71	33.28	59.37	31.24	0.015
	48x32	P2	0.047388	7.3942	6.4497	7.2007	6.7764	62.432	32.651	58.957	30.768	0.028
	72x48	P2	0.047744	7.38451	6.46086	7.19820	6.78725	61.2695	32.2765	58.1199	30.5122	0.067
	96x64	P2	0.047867	7.38176	6.46459	7.19722	6.79115	60.8708	32.1475	57.8245	30.4281	0.129
	ext.	—	0.048024	7.3787	6.4692	7.1959	6.7962	60.364	31.983	57.443	30.324	—
HG	29x21	P2	0.050	7.37	6.53	7.26	6.69	62.4	31.2	61.0	30.4	3.6
	39x25	P2	0.0488	7.37	6.47	7.20	6.74	61.3	31.8	58.9	30.4	1.6
Ko	16x16	P1	0.0226	6.947	6.384	—	—	50.40	32.65	—	—	2.
	24x16	P1	0.0268	6.88	6.33	—	—	48.27	33.36	—	—	4.
Mo	48x32	chaotic		—	—	—	—	—	—	—	—	0.0175
	96x64	P4	.0961924	7.36751	6.49684	7.26605	6.83458	61.2196	31.8696	59.4829	30.2926	
				7.35690	6.37794	7.07543	6.72420	59.4645	32.3208	55.0453	30.4943	.7
	192x128	P4	.0960978	7.36708	6.48274	7.23434	6.81736	60.9105	31.9008	58.7431	30.2672	
				7.36128	6.40786	7.11429	6.74776	59.8013	32.1912	55.9230	30.3964	3.2
	384x256	P2	.0485805	7.348633	6.454025	7.184493	6.753839	60.35083	31.77670	57.69152	30.22963	18.0
SM	21x21	P1	0.0273	7.255	6.600	—	—	55.80	30.86	—	—	0.056
	31x31	P2	0.0508	7.31	6.45	7.14	6.75	60.3	31.46	55.5	29.95	0.167
	41x41	P2	0.0494	7.321	6.422	7.130	6.764	60.5	31.86	56.0	30.00	?

Table 8a: Same quantities as in table 8 for case 3' (Ra=218000)

Code	Grid	Type	Period	Nusselt Nu. max	Nusselt Nu. min	velocity(rms) max	velocity(rms) min	max	min
Ch	24x16	P2	0.047800	7.4233	6.4880	7.2239	6.8356	60.580	32.146	57.483	30.412
	36x24	P4	0.095510	7.4018	6.5084	7.2525	6.8469	60.953	32.030	58.574	30.393
				7.3973	6.4504	7.1597	6.7930	60.100	32.259	56.401	30.492
Ha	48x32	P4	0.094205	7.4049	6.4944	7.2719	6.8308	63.215	32.667	60.732	30.846
				7.4058	6.4217	7.1397	6.7524	61.986	32.962	57.401	30.985
	96x64	P4	0.095126	7.3947	6.5028	7.2536	6.8388	61.518	32.195	59.153	30.512
				7.3915	6.4388	7.1480	6.7768	60.541	32.449	56.620	30.624
SM	41x41	P4?	0.0979	7.3286	6.5156	7.2647	6.8440	61.73	31.59	59.25	30.07
				7.3403	6.3808	7.0453	6.7131	59.85	32.17	53.81	30.31

difference points, finite elements or Fourier modes. We like to point out that N is not necessarily identical with the degrees of freedom in the system to be solved, which can, especially for finite element methods, be higher by a factor of about 2–4. Not surprisingly, those codes which use mesh refinement in the boundary layers already came closer with a smaller number of elements or difference points. This also holds for FD methods, where non-equidistant mesh spacing is less common. It is remarkable that for Nu and v_{rms} several extrapolated results (by the Romberg or Aitken method) agree within 5 or more digits.

For the local temperature gradients and extrema the variance among results is somewhat larger, especially for high Rayleigh numbers. For example, for the value of q_1, the range of the reported 'best' values spans ±20 per cent. Partially, the reason could be that usually less attention is paid to these quantities as compared to the Nusselt number, and therefore less effort was spent on an accurate determination. However, another reason is certainly also that local values are more prone to numerical error than global averages.

Five workers contributed geoid and topography data for the constant viscosity cases (seven, counting Ch, Ko and Ch', Ko' separately). Despite the difficulties in determining these quantities, the agreement is satisfactory for all Rayleigh numbers. Ch finds that the kernel method (Ch') gives better results on coarse grids than evaluating the normal stress at boundaries by differentiation. The topography values reported by Ko differ slightly from the other solutions. This is due to a different normalization, i.e. setting the mean dynamical pressure at the surface rather than the mean topography to zero. The peak-to-peak

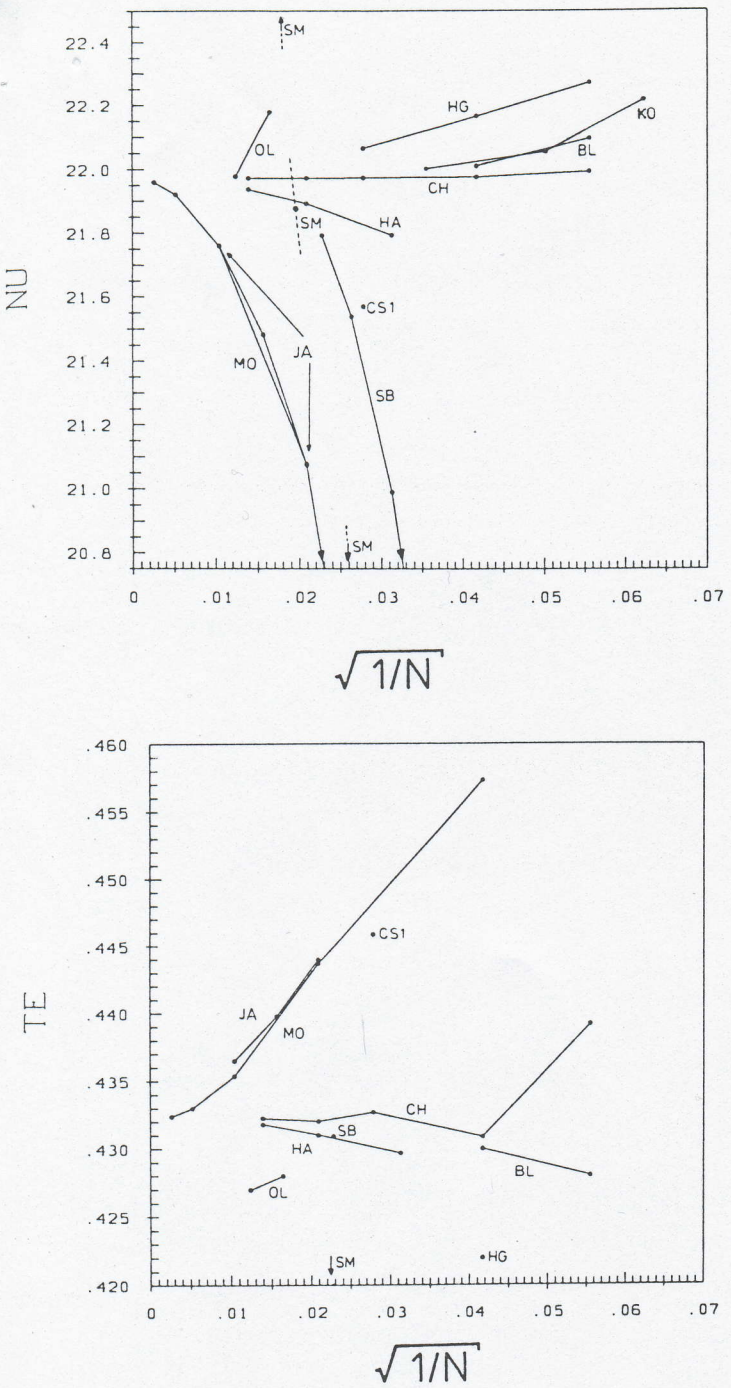

Figure 1. (a) Nusselt numbers versus grid size for case 1(c) ($\mathrm{Ra} = 10^6$). The gridsize is characterized by $\sqrt{N^{-1}}$, where N is the number of finite difference points, number of elements or number of Fourier modes. For labels see Table 2. (b) Local temperature extremum T_e versus grid size.

amplitude ($\xi_1 - \xi_2$), which is unaffected by the difference in normalization, agrees well with the other solutions.

Isotherms, stream lines, topography and geoid of the two variable viscosity cases are displayed in Figs 2–5. The plots are obtained from a high-resolution study; however, we do not mean to use these contour drawings as standards, but include them here for illustration only. Due to temperature-dependent viscosity the upper boundary layer is spanned by a larger temperature jump than the lower one, while the addition of pressure dependence reverses this tendency. Topography on the surface boundary is larger than at the bottom boundary with temperature dependence; here again including the pressure dependences reverses the effect. Particularly interesting is the geoid signature in case 2(b), where a local minimum is found over both the upwelling and downwelling currents.

Not unexpectedly, the scatter of results is slightly larger than for the simpler constant viscosity cases. Still, Nusselt number and rms velocity generally agree within some per

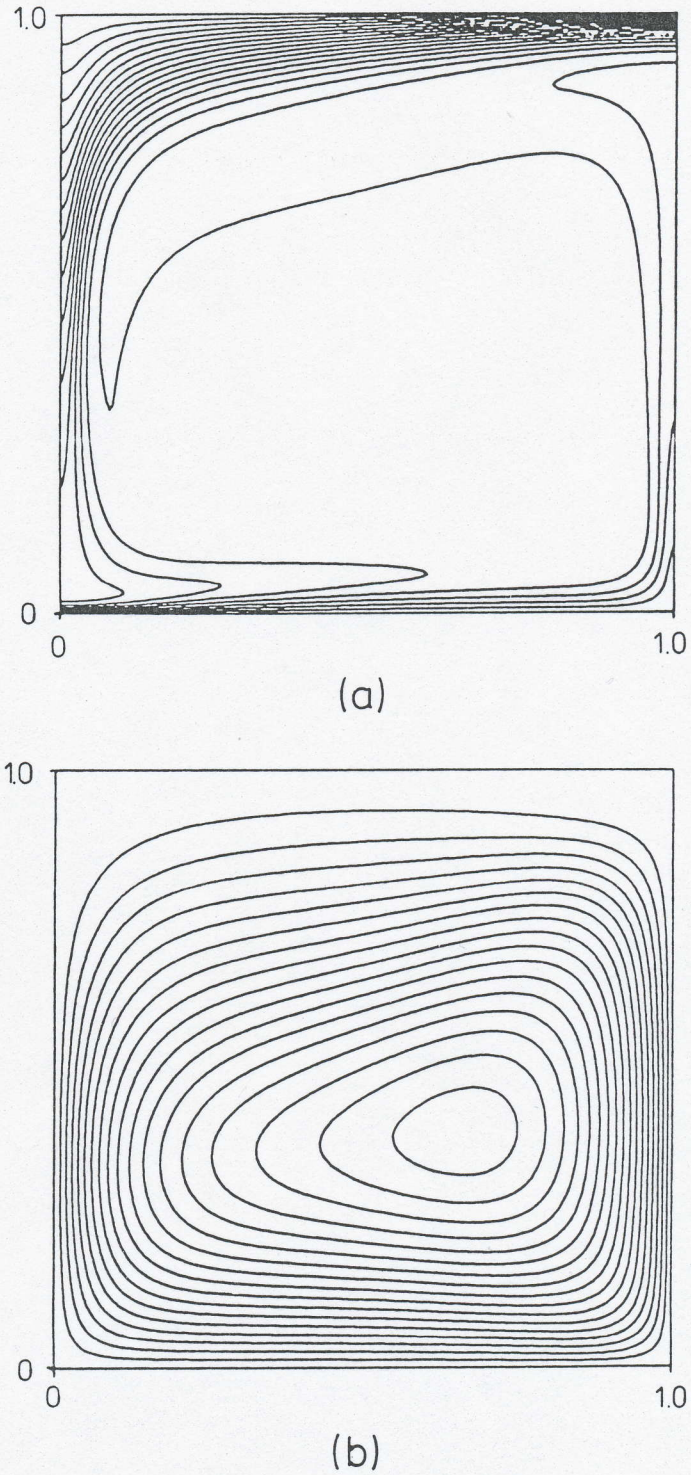

Figure 2. Isotherms (a) and streamlines (b) for case 2(a). Contour lines are equally spaced with $\Delta T = 1/20$ and $\Delta\psi = 10$. Note that contrary to the convention in the rest of this report the upwelling flow is on the right.

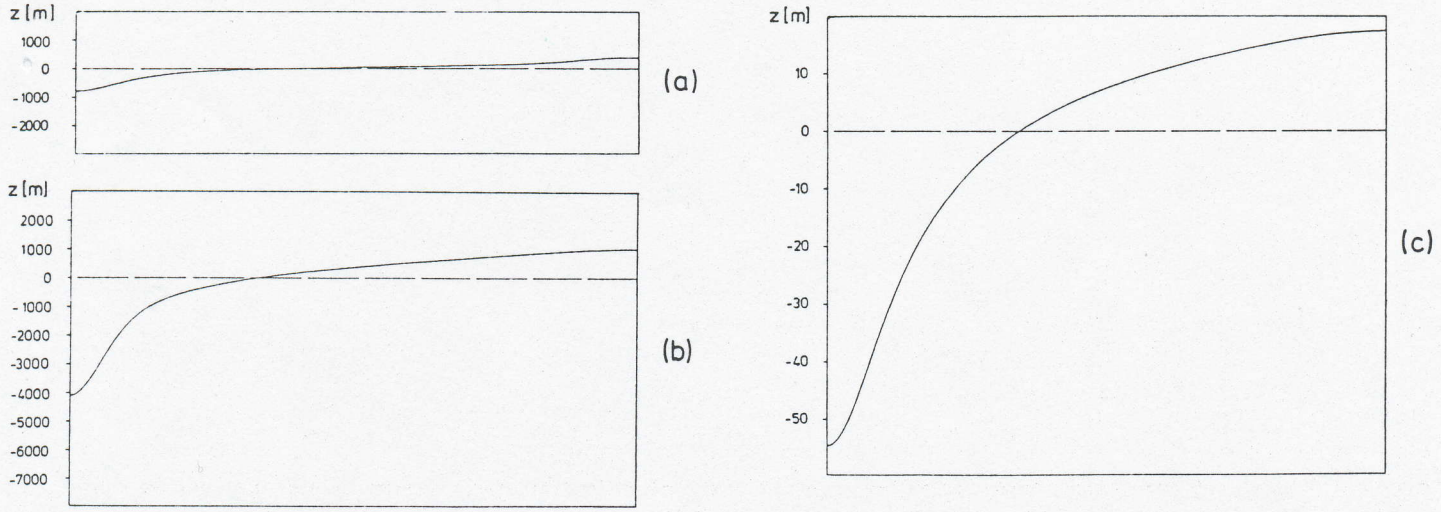

Figure 3. Bottom (a), surface topography (b) and geoid (c) for case 2(a). The upwelling flow is to the right.

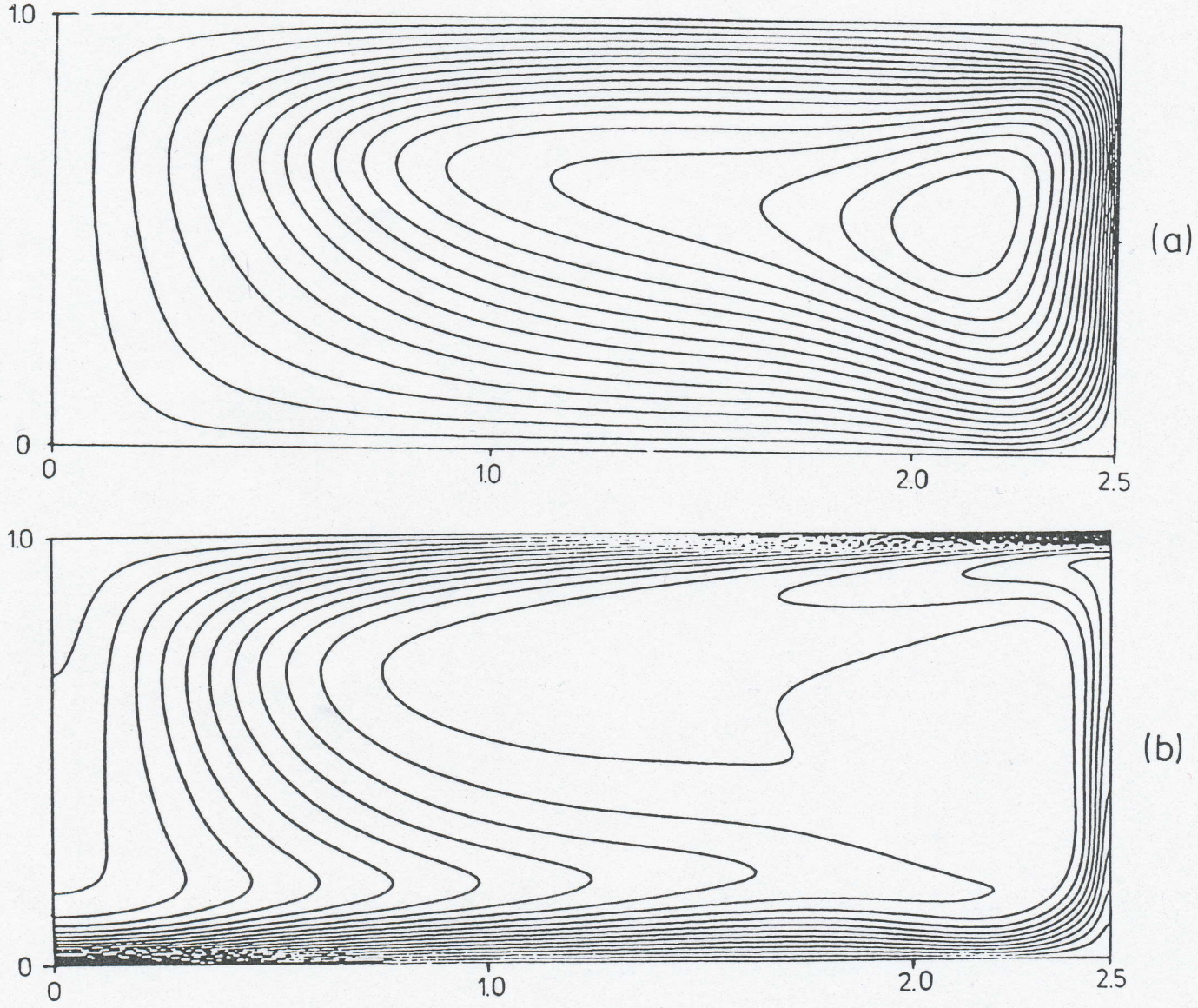

Figure 4. Streamlines (a) and isotherms (b) for case 2(b). Contour lines are equally spaced with $\Delta T = 1/20$ and $\Delta\psi = 5$.

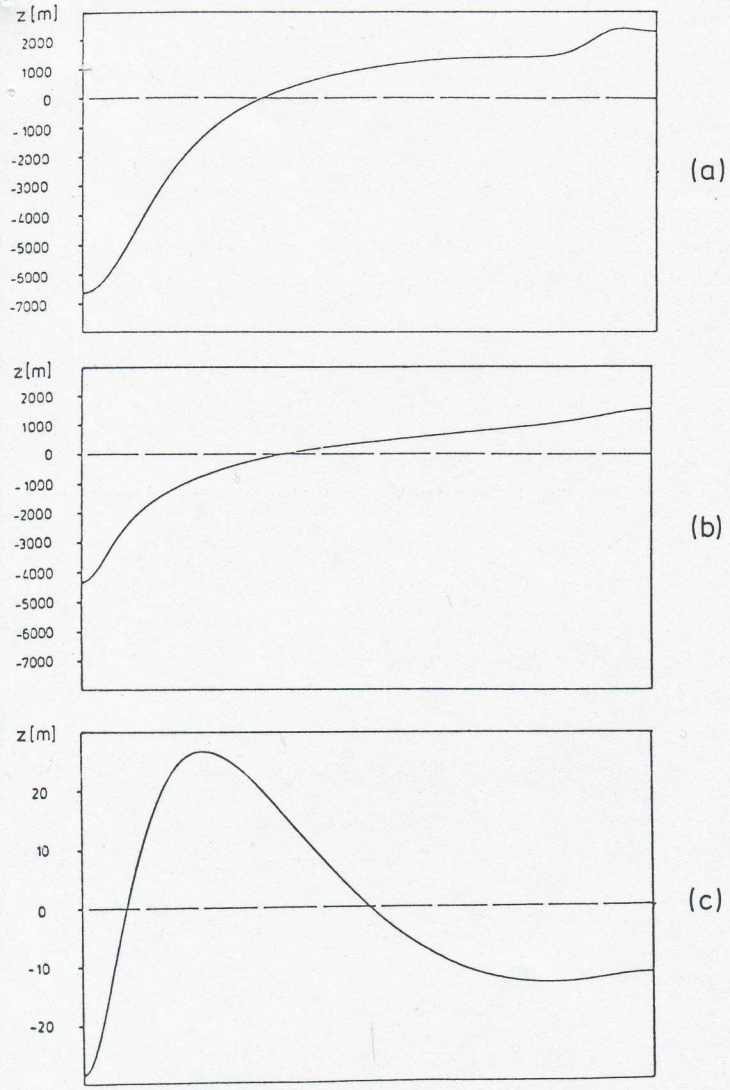

Figure 5. Bottom (a), surface topography (b) and geoid (c) for case 2(b). The upwelling flow is to the right.

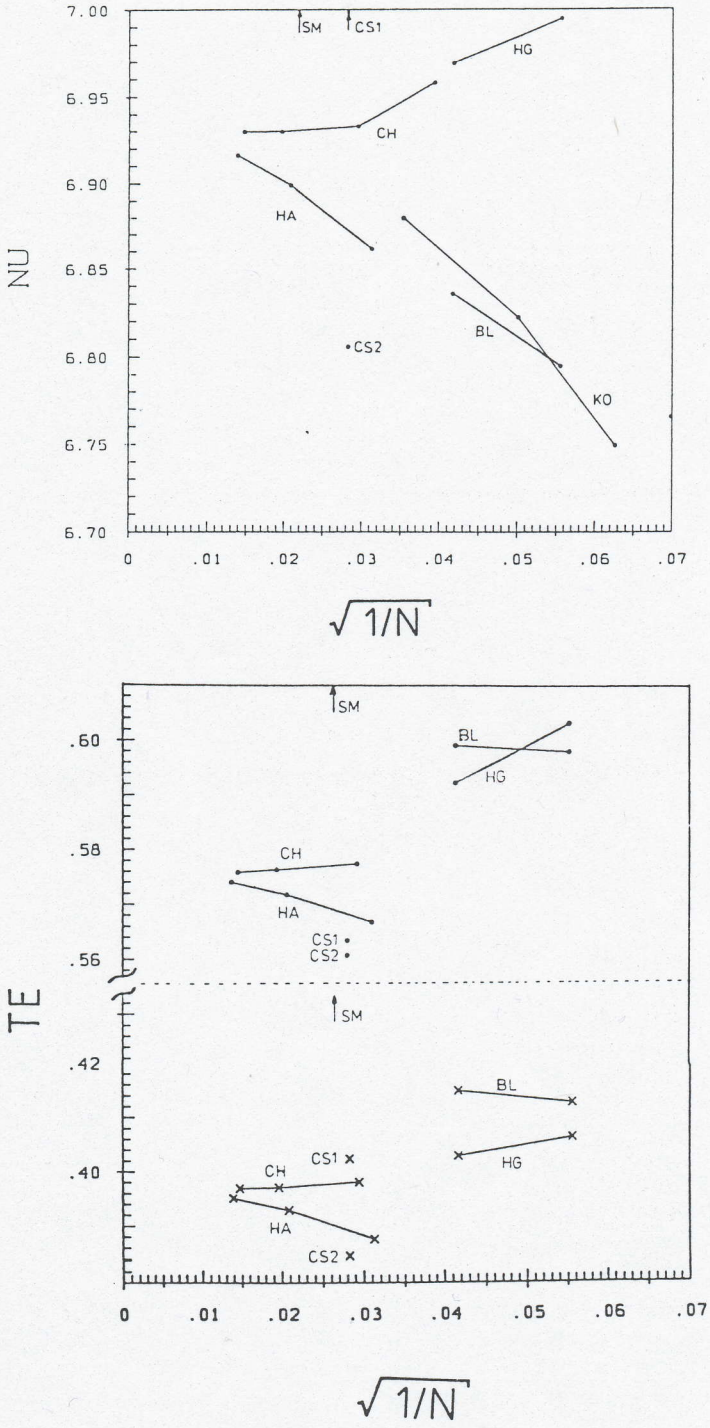

Figure 6. (a) Nusselt number vs. gridsize for case 2(b) (temperature- and pressure-dependent viscosity). (b) Local temperature extrema T_e versus grid size. Dots denote the extremum near the upper and crosses near the lower boundary layer.

cent for all reported 'best' results (Fig. 6). Cs finds that his results are more accurate when using central differences (Cs2) rather than upwind differencing (Cs1). Topography and geoid are more problematic in the variable viscosity cases. The geoid data calculated by Ch, Ha and Ko agree well, also the topography data, apart from the problem of the different normalization used by Ko. After changing the path of horizontal integration of the Navier–Stokes equation to a mid-depth level (see Section 3), SM comes close to other contributions. These data are reported in Tables 6(b) and 7(b) under the entry SM. Integration along the outer boundaries yielded no convergent solution at all in their case, which is likely to be due to the strong viscosity gradients and the use of an equispaced grid. Ch and Ha also report (with non-equispaced grids) inferior results with this choice of integration path.

In the time-dependent case 3, the correct solution is most probably a P2 cycle. All contributors except Cs1 and Ko end up with a P2 cycle at the highest degree of resolution that they employed (Table 8). This applies for codes which seem to underestimate the degree of complexity in the temporal behaviour on coarse grids (Ch, SM) as well as for those which overestimate it (Ha, Mo). It is interesting that there does not seem to be a general rule as to the kind of behaviour with insufficient resolution, contrary to the previous assumption that under-resolution generally leads to more complex dynamical behaviour. Time-series plots of Nu and v_{rms}, and a phase space projection of the P2 cycle are shown in Fig. 7. In cases where a P2 cycle was obtained, the reported extrema of Nu and v_{rms} agree well, likewise the period of the oscillations. Three contributions for a Rayleigh number of 218 000 (case 3′) agree on a P4 cycle. Because two of those codes show a tendency to underestimate the

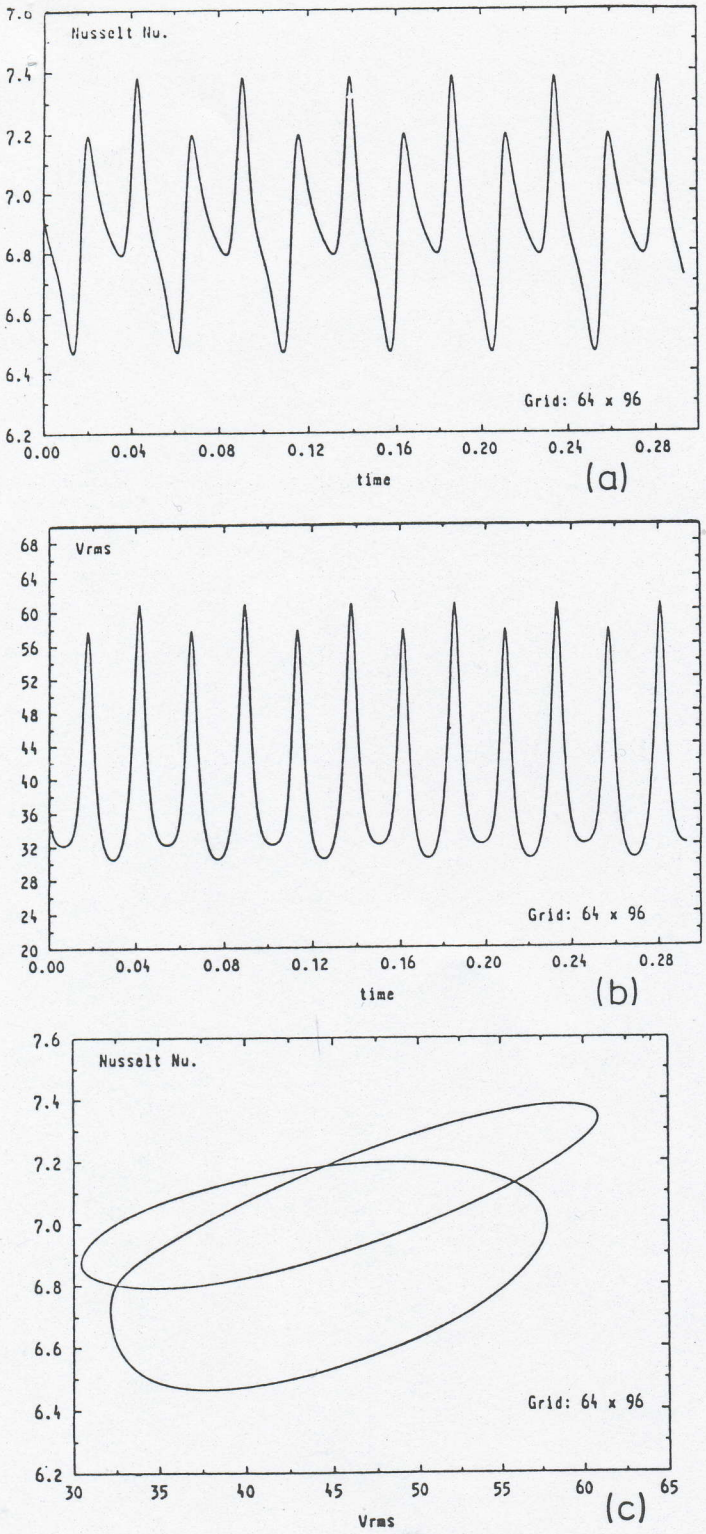

Figure 7. (a) Time-series plots of the Nusselt number; (b) rms-velocity; (c) Phase space cut, spanned by the Nusselt number and the rms velocity for case 3, showing the P2 structure of the limit cycle.

degree of complexity, it is quite certain that the bifurcation point P2–P4 lies in between the Rayleigh numbers 216 000 and 218 000.

5 BEST ESTIMATE OF SOLUTIONS

We have tried to determine a best estimate of the solutions and the uncertainty of these values (Table 9). We recommend the use of these data for validation of convection codes. For each datum a few individual results have been selected to define the 'best value'. We wish to emphasize that we do not imply any superiority of the respective codes compared to others. The reason for their selection has been that the maximum achieved resolution was better than in other contributions, and that results were obtained on at least three or four successively refined grids, which often allowed a reliable extrapolation. Thus, the choice of these contributions may reflect more the availability of computer time rather than quality of codes.

The criteria for defining the 'best value' were the following. We require a close agreement of 'best individual values' (most extrapolated), from three or more sufficiently distinct methods, if possible. Next best is when two distinct codes yield very close values, and when there is at least one further contribution, which does not achieve the same level of accuracy due to lower resolution, but in principal corroborates the correctness of the other two results. This is a safeguard against a common systematic error in the first two codes, for which there might be a small chance. In the worst case, we have only two results in good agreement with little support from other contributors. In Table 9 those contributions which were taken to define the best estimate are underlined, while additional supporting solutions are not. We would like to point out that the results of Ch and Ha, although coming from the same institute, were obtained independently with entirely different codes.

Additional information not presented in this report has been used to determine the most likely value out of the two, three or four individual data taken to define the best estimate. Mainly, these are the data from the Romberg extrapolation tableau (Ha, Mo) or the plausibility of the exponent obtained by the Aitken extrapolation scheme (Ch). Ch had also provided additional information from solutions obtained on differently structured grids with the same number of elements.

The quoted uncertainties of the best values are conservative; the true solution may often be much closer than the error values suggest. Our criterion for fixing the uncertainty level was that all the two to four data defining our best value had to lie within this range. Of course, occasionally the agreement between them may be fortuitous, especially if there are only two values available. Therefore, we estimated the quality of the extrapolations with the data mentioned above, also considering the 'distance' over which the extrapolation was carried out and determined the uncertainty range accordingly. In most cases one 'real' (not extrapolated) result lies inside the error range. If there were only two data available a larger allowance has been made than in the cases where we had three or more.

6 CONCLUSION

Our benchmark comparison shows a satisfactory agreement among all partaking numerical codes concerning most of the requested quantities. The tabulated material is helpful to indicate the necessary resolution to obtain the desired accuracy for different types of codes. Increased resolution in the boundary layers of high Rayleigh number convection gives better results than equidistant mesh spacing, when the same number of grid points (elements) is used. Global averages (Nu, v_{rms}) are usually more accurately determined than local values. High-resolution studies, together with an

Table 9 Best estimates and uncertainty of solutions

Quantity	Value	Uncertainty	Codes	
Case 1a				
Nu	4.884409	0.000010	Ch, Mo, SB	Ha, HG
V_{rms}	42.864947	0.000020	Ch, Ha, Mo, SB	
q_1	8.059384	0.000003	Ch, Ha, Mo, SB	
q_2	0.588810	0.000003	Ch, Mo, SB	Ha
T_c	0.422162	0.000010	Ch, Mo, SB	Ha, Ja
Z_c	0.224903	0.000100	Ha, Mo	Ch, SB
ξ_1	2254.022	0.050	Ch, Ha	Ja, SM
ξ_2	-2903.230	0.050	Ch, Ha	Ja, SM
$x(\xi=0)$	0.539372	0.000030	Ch, Ha	Ja, SM
ϕ_1	54.8218	0.0020	Ch, Ha	SM
ϕ_2	-62.6225	0.0020	Ch, Ha	SM
$x(\phi=0)$	0.519639	0.000030	Ch, Ha	SM
Case 1b				
Nu	10.534095	0.000010	Ch, Ha, Mo	SB, HG
V_{rms}	193.21454	0.00010	Ch, Ha, Mo	SB, Ko
q_1	19.079440	0.000040	Ch, Ha, Mo	SB
q_2	0.722751	0.000020	Ch, Mo	Ha, SB
T_c	0.428427	0.000015	Ch, Mo, SB	Ha, Ja
Z_c	0.111804	0.000200	Ch, Mo	Ha, SB
ξ_1	1460.99	0.10	Ch, Ha	Ja
ξ_2	-2004.20	0.10	Ch, Ha	Ja
$x(\xi=0)$	0.529330	0.000030	Ch, Ha	Ja
ϕ_1	27.7025	0.0030	Ch, Ha	SM
ϕ_2	-32.0150	0.0040	Ch, Ha	SM
$x(\phi=0)$	0.512290	0.000030	Ch, Ha	SM
Case 1c				
Nu	21.972465	0.000020	Ch, Mo	Ha,HG,Ja,Ko
V_{rms}	833.98977	0.00020	Ch, Mo	Ha, Ko
q_1	45.96425	0.00030	Ch, Ha	Mo, HG
q_2	0.877170	0.000010	Ch, Mo	Ha, HG
T_c	0.432202	0.000100	Ch, Mo	Ha, Ja
Z_c	0.057740	0.000050	Ch, Mo	Ha
ξ_1	931.96	0.10	Ch, Ha	Ja
ξ_2	-1283.80	0.10	Ch, Ha	Ja
$x(\xi=0)$	0.50649	0.00005	Ch, Ha	Ja
ϕ_1	13.451	0.050	Ch, Ha	Ko, SM
ϕ_2	-15.0033	0.080	Ch, Ha	Ko, SM
$x(\phi=0)$	0.50042	0.00010	Ch, Ha	Ko
Case 2a				
Nu	10.0660	0.00020	Ch, Ha	Cs, HG
V_{rms}	480.4334	0.1000	Ch, Ha	Ko, Sm
q_1	17.53136	0.00400	Ch, Ha	HG
q_2	1.00851	0.00020	Ch, Ha	HG
q_3	26.8085	0.0100	Ch, Ha	
q_4	0.497380	0.000100	Ch, Ha	
T_c	0.7405	0.0005	Ch, Ha	HG
Z_c	0.06233	0.00020	Ch, Ha	HG
T_c	0.8323	0.0005	Ch, Ha	
Z_c	0.8243	0.0020	Ch, Ha	Cs, HG
ξ_1	1010.92	0.20	Ch, Ha	SM
ξ_2	-4098.09	0.80	Ch, Ha	SM
$x(\xi=0)$	0.67700	0.00005	Ch, Ha	SM
ξ_3	386.38	0.10	Ch, Ha	
ξ_4	-788.10	0.50	Ch, Ha	
$x(\xi=0)$	0.63084	0.00020	Ch, Ha	
ϕ_1	17.346	0.010	Ch, Ha	Ko,SM
ϕ_2	-54.600	0.020	Ch, Ha	Ko, SM
$x(\phi=0)$	0.65993	0.00010	Ch, Ha	Ko, SM

Table 9 (contd.)

Case 2b				
Nu	6.9299	0.0005	Ch, Ha	HG, Ko
V_{rms}	171.755	0.020	Ch, Ha	HG, Ko
q1	18.4842	0.0100	Ch, Ha	HG
q2	0.17742	0.00003	Ch, Ha	HG
q3	14.1682	0.0050	Ch, Ha	HG
q4	0.61770	0.00005	Ch, Ha	
T_c	0.3970	0.0008	Ch, Ha	
Z_c	0.1906	0.0010	Ch, Ha	
T_c	0.57584	0.00050	Ch, Ha	
Z_c	0.7837	0.0030	Ch, Ha	HG
ξ_1	1538.8	3.0	Ch, Ha	SM
ξ_2	-4341.5	1.5	Ch, Ha	SM
x (ξ = 0)	1.6358	0.0030	Ch, Ha	SM
ξ_3	2311.8	1.0	Ch, Ha	SM
ξ_4	-6639.7	3.0	Ch, Ha	SM
x (ξ = 0)	1.7311	0.0005	Ch, Ha	SM
ϕ_1	-11.80	0.30	Ch, Ha	Ko, SM
ϕ_2	-28.25	0.30	Ch, Ha	Ko, SM
x(ϕ= 0)	1.2745	0.0010	Ch, Ha	Ko, SM
x(ϕ = 0)	2.3065	0.0020	Ch, Ha	Ko, SM
Case 3				
Period	0.04803	0.00003	Ch, Ha	HG
Nu_{max}	7.379	0.005	Ch, Ha	HG, Mo
Nu_{min}	6.468	0.005	Ch, Ha	HG, Mo
Nu_{max}	7.196	0.005	Ch, Ha	HG, Mo
Nu_{min}	6.796	0.005	Ch, Ha	HG, Mo
v_{max}	60.367	0.015	Ch, Ha	Mo
v_{min}	31.981	0.020	Ch, Ha	Mo
v_{max}	57.43	0.05	Ch, Ha	Mo
v_{min}	30.32	0.03	Ch, Ha	Mo

extrapolation of results, allows us to pin down the 'correct' solution with fairly low levels of uncertainty. We propose that these values are used for the validation of mantle convection codes.

ACKNOWLEDGMENTS

We gratefully acknowledge financial support by the Stiftung Volkswagenwerk for the workshop on mantle convection held at Neustadt in 1987 June.

DM was a recipient of a Visiting Scientist appointment at the Institute of Naval Oceanography for the year 1987/88. INO is sponsored by the US Navy and is administered by the Office of the Chief of Naval Research. MK has been supported by the Florida State University Supercomputer Computations Research Institute which is partly funded by the U.S. Department of Energy through contract No. DE-FC05-85ER25000.

REFERENCES

Busse, F. H., 1967. On the stability of two-dimensional convection in a layer heated from below, *J. math. Phys.*, **46,** 140–150.

Christensen, U., 1984. Convection with pressure- and temperature-dependent non-Newtonian rheology, *Geophys. J. R. astr. Soc.*, **77,** 343–384.

Cserepes, L., 1985. On different numerical solutions of the equations of mantle convection, in *Annales Universitatis Scientiarum Budapestinensis,* Section of Geophysics and Meteorology, pp. 52–67, ed. Stegena, L., Eötvös Univesity, Budapest.

Davis, G. F., 1986. Mantle convection under simulated plates: effects of heating modes and ridge and trench migration, and implications for the core-mantle boundary, bathmetry, the geoid and Benioff Zones, *Geophys. J. R. astr. Soc.*, **84,** 153–183.

de Vahl-Davies, G. & Jones, I. P., 1983. Natural convection in a square cavity: a comparison exercise, *Int. J. num. Meth. Fluids,* **3,** 227–248.

Dongara, J. J., 1986. Performance of various computers using standard linear equations software in a Fortran environment, Technical Memorandum No. 23, Argonne National Laboratory, 9700, South Cass Avenue, Argonne, IL 60349, USA.

Gartling, D., 1977. NACHOS—A finite element computer program for incompressible flow problems, Parts I and II, Sand 77-1333, Sand 77-1334, Sandia National Laboratories, Albuquerque, NM, USA.

Hansen, U. & Ebel, A., 1984. Experiments with a numerical model related to mantle convection: boundary layer behaviour of small and large-scale flows, *Phys. Earth planet. Inter.*, **36,** 374–390.

Lennie, T. B., McKenzie, D. P., Moore, D. R. & Weiss, N. O., 1988. The breakdown of steady convection, *J. fluid Mech.*, **188,** 47–85.

McKenzie, D. P., Roberts, J. M. & Weiss, N. O., 1974. Convection in the earth's mantle: towards a numerical simulation, *J. fluid Mech.*, **62,** 465–538.

Moore, D. R., Peckover, R. R. & Weiss, N. O., 1974. Difference methods for two-dimensional convection, *Computer Phys. Communs,* **6,** 198–220.

Parsons, B. & Daly, S., 1983. The relationship between surface topography, gravity anomalies, and temperature structure of convection, *J. geophys. Res.*, **88,** 1129–1144.

Schmeling, H. & Jacoby, W. R., 1981. On modelling the lithosphere in mantle convection with non-linear rheology, *J. Geophys.*, **50,** 89–100.